Epigenetic changes during disease progression in a murine model of human chronic lymphocytic leukemia

Shih-Shih Chen[a,b,c], Aparna Raval[a,d], Amy J. Johnson[c], Erin Hertlein[c], Te-Hui Liu[a,e], Victor X. Jin[a], Mara H. Sherman[f], Shu-Jun Liu[c], David W. Dawson[e], Katie E. Williams[b], Mark Lanasa[g], Sandya Liyanarachchi[a], Thomas S. Lin[b], Guido Marcucci[a,b], Yuri Pekarsky[a], Ramana Davuluri[a], Carlo M. Croce[a], Denis C. Guttridge[a], Michael A. Teitell[f], John C. Byrd[a,c,1,2], and Christoph Plass[a,h,1,2]

[a]Department of Molecular Virology, Immunology, and Medical Genetics, Human Cancer Genetics Program, the Comprehensive Cancer Center, [b]Department of Molecular Genetics, [c]Division of Hematology-Oncology, Department of Medicine, Ohio State University, Columbus, OH 43210; [d]Department of Oncology, CCSR 2250, Stanford University, Stanford, CA 94305; [e]Department of Infectious Disease, The Children's Hospital of Philadelphia, Philadelphia, PA 19104; [f]Molecular Biology Institute, Department of Pathology and Laboratory Medicine, Broad Stem Cell Research Center, and Jonsson Comprehensive Cancer Center, University of California, Los Angeles, CA 90095; [g]Department of Medicine, Division of Medical Oncology, Duke University Medical Center, Durham, NC 27710; and [h]Division of Epigenomics and Cancer Risk, German Cancer Research Center, 69120 Heidelberg, Germany

Communicated by Albert de la Chapelle, Ohio State University, Columbus, OH, June 17, 2009 (received for review March 1, 2009)

Epigenetic alterations, including gain or loss of DNA methylation, are a hallmark of nearly every malignancy. Changes in DNA methylation can impact expression of cancer-related genes including apoptosis regulators and tumor suppressors. Because such epigenetic changes are reversible, they are being aggressively investigated as potential therapeutic targets. Here we use the Eμ-TCL1 transgenic mouse model of chronic lymphocytic leukemia (CLL) to determine the timing and patterns of aberrant DNA methylation, and to investigate the mechanisms that lead to aberrant DNA methylation. We show that CLL cells from Eμ-TCL1 mice at various stages recapitulate epigenetic alterations seen in human CLL. Aberrant methylation of promoter sequences is observed as early as 3 months of age in these animals, well before disease onset. Abnormally methylated promoter regions include binding sites for the transcription factor FOXD3. We show that loss of *Foxd3* expression due to an NF-κB p50/p50:HDAC1 repressor complex occurs in TCL1-positive B cells before methylation. Therefore, specific transcriptional repression is an early event leading to epigenetic silencing of target genes in murine and human CLL. These results provide strong rationale for the development of strategies to target NF-κB components in CLL and potentially other B-cell malignancies.

CLL | DNA methylation | epigenetics | FOXD3

Epigenetic alterations in cancer receive great attention since their contributions to tumor development and progression have now been documented (1). Major questions in the field relate to formation of global patterns of epigenetic alterations, the mechanisms that lead to epigenetic changes and the role of target genes in healthy tissues (2). Epigenetics, or the inheritance of gene expression patterns through mechanisms that do not change the DNA sequence, were initially investigated by measurement of DNA methylation occurring at cytosine residues. However, it is also clear that additional epigenetic factors such as histone tail modifications or small RNAs cooperate in the epigenetic regulation of genes (3, 4). DNA methylation in mammals occurs predominantly at cytosine residues, creating a 5-methylcytosine. The covalent addition of a methyl group to cytosine is stable from fixation processes and therefore allows high-throughput genome-wide or gene-specific quantification of DNA methylation on archived samples (5).

DNA methylation abnormalities, especially gain of methylation in normally unmethylated promoter or other regulatory regions (hypermethylation) or loss of methylation in normally methylated repetitive sequences (hypomethylation), have been described for almost all human tumor types as well as tumors from animal models, suggesting a general mechanism in cancer that leads to aberrant DNA methylation. However, there is evidence that individual patterns of aberrant methylation are tumor-type specific and non-random, thus arguing for additional tissue-specific mechanisms (6). Based on in vitro studies, several groups have put forward mechanisms of methylation specificity, postulating the recruitment of DNA methyltransferases (DNMTs) to target sites by oncogenes or sequence-specific methylation events (7). However in vivo experiments have been unable to confirm these hypotheses.

Similarly unclear is the timing of aberrant DNA methylation events. There is evidence that epigenetic alterations could precede the initiation of tumorigenesis as exemplified by the recent discoveries of epimutations in *MLH1* or *MSH2* predisposing to colorectal cancer (8), or the loss of DNMT1 activity in mouse models developing T-cell lymphoma (9). However, these examples seem to be more the exception than the rule, leaving room for more general and still undiscovered mechanisms. Evidence for DNA methylation as an early event in transformation comes from studies of clinical samples in lung and colon cancer, where DNA methylation changes were detected in early preneoplastic lesions (10).

Chronic lymphocytic leukemia (CLL) is characterized by gradually increasing levels of malignant B cells in the bone marrow, lymphoid organs and circulation that are resistant to the normal process of apoptosis. Recently, a transgenic mouse model of CLL was generated by introducing the human *TCL1* gene under control of a B cell-specific Ig promoter and Eμ enhancer (11). TCL1 transgenic mice develop a monoclonal B-cell lymphocytosis that is very similar to human CLL in immunophenotypic and clinical features as well as response to fludarabine, a commonly used agent in this disease (12). In this study, we investigated epigenetic alterations in this CLL mouse model at various times before development of disease. We demonstrate that DNA methylation changes occur early in disease development and recapitulate alterations seen in human

Author contributions: S.-S.C., A.J.J., E.H., J.C.B., and C.P. designed research; S.-S.C., T.-H.L., V.X.J., M.H.S., S.-J.L., and K.E.W. performed research; D.W.D., M.L., T.S.L., G.M., Y.P., C.M.C., D.C.G., and M.A.T. contributed new reagents/analytic tools; S.-S.C., A.R., S.L., R.D., J.C.B., and C.P. analyzed data; and S.-S.C., J.C.B., and C.P. wrote the paper.

The authors declare no conflict of interest.

[1]J.C.B. and C.P. contributed equally to the work

[2]To whom correspondence may be addressed. E-mail: john.byrd@osumc.edu or c.plass@dkfz-heidelberg.de.

This article contains supporting information online at www.pnas.org/cgi/content/full/0906455106/DCSupplemental.

GENETICS

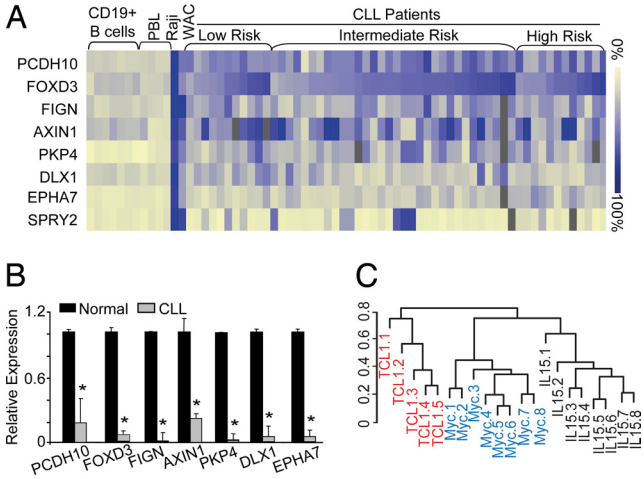

Fig. 1. Specific DNA methylation profiling in Eμ-TCL1 mice recapitulates the changes in CLL patients. (*A*) MassARRAY analysis on CD19+ B cells, peripheral blood lymphocytes (PBL), Raji, WaC3CD5, and CLL B-cell samples. Each row represents a gene and each column indicates a sample. The heat map presents the quantitative methylation data from 0% to 100%. (*B*) Quantitative PCR results on CD19+ B-cell samples ($n = 4$) and CLL patients ($n = 30$). The expression level in the normal CD19+ B-cell samples was defined as 1. Error bars, s.e.m. ($P \leq 0.028$ by Student t test). (*C*) Hierarchical cluster analysis with 5 TCL1 CLL leukemia, 8 Myc T/NK cell leukemia and 8 IL15 T cell leukemia mice, using all of the spots with at least 1 methylation (1,491 spots) across samples.

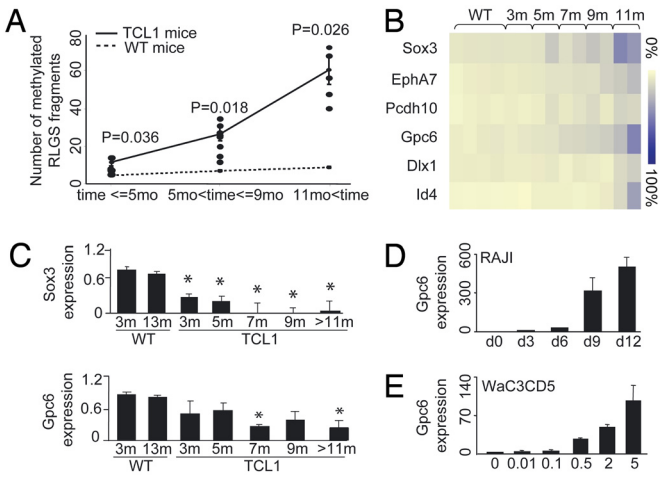

Fig. 2. Early and accumulating DNA methylation in Eμ-TCL1 mice. (*A*) Average overall CpG methylation in TCL1 mice at 3, 5, 7, and 9 months ($n = 3$) and mice with advanced CLL ($n = 5$) as compared to WT mice at 4, 8, and 11 months ($n = 2$). *P* values given were calculated by Wilcoxon test. The significance of increased DNA methylation frequency overtime was calculated by Jonckheere-Terpstra test ($P = 4.701e\text{-}06$). (*B*) MassARRAY results of splenic B cells from WT ($n = 4$) or TCL1 mice ($n = 2$ for each age). (*C*) Expression of early methylated *Sox3* and *Gpc6* genes in TCL1 mouse splenic B cells compared to 3-month-old WT mice by SYBR-green PCR ($n = 3$, $^*P < 0.01$ by Student t test). (*D*) Progressive re-activation of *GPC6* expression after 0.5 μM 5aza-dC treatment over 12 days in Raji B-lymphoblastoid cells. (*E*) Increased expression of *GPC6* in WaC3CD5 CLL cells treated dose-escalating concentrations (μM) of 5aza-dC for 3 days. The expression level of *GPC6* was plotted relative to the expression level in the day 0 or 0 μM 5aza-dC amplified samples, respectively. Error bars, s.d.

CLL. Furthermore, our studies implicate silencing of transcription factor *FOXD3* as a key event early in leukemogenesis in both mouse and human CLL.

Results

Disease-Specific DNA Methylation in Eμ-TCL1 CLL Progression Recapitulates Epigenetic Alterations of Human CLL. Human CLL has been characterized as having multiple epigenetic defects that include abnormal methylation and silencing of genes. One oncogene, TCL1, is generally over-expressed in CLL and is associated with poor response to therapy (13). The Eμ-TCL1 transgenic mouse model of CLL shows characteristics similar to the human disease, with an initial expansion of non-clonal B lymphocytes at approximately 3 months followed by progression to a mature B-cell leukemia at 9–11 months (11). Due to the similarities of human CLL and Eμ-TCL1 murine leukemia, we hypothesized that aberrant epigenetic changes might also occur in the Eμ-TCL1 mice and that the timing of such changes may provide valuable information both on CLL biology and on early targets for therapeutic intervention.

Genome-wide CpG hypermethylation was therefore evaluated in this model using restriction landmark genomic scanning [RLGS (14)]. Cells obtained from spleens from Eμ-TCL1 mice at 11–14 months, the age of leukemia onset, were compared to cells from spleens of age-matched wild-type (WT) mice. After eliminating 522 polymorphic fragments and 6 age-dependent methylation events, a total of 1,491 RLGS fragments were scored. An overall increase in DNA methylation was found in the spleen cells from Eμ-TCL1 mice with symptomatic disease, ranging from 2.5% to 5.5% of all evaluated RLGS fragments. These frequencies of promoter methylation are comparable to the frequencies previously reported for human CLL (2.5–8.1%) which was significantly higher than age matched normal B cells (15). Table S1 provides the list of methylated RLGS fragments in the Eμ-TCL1 mice. Among these methylated genes, 8 randomly selected genes (*PCDH10*, *FOXD3*, *FIGN*, *AXIN1*, *PKP4*, *DLX1*, *EPHA7*, and *SPRY2*) were investigated by MassARRAY (16) and by real-time RT-PCR in 55 samples from CLL patients. Interestingly, 7 of the 8 genes (all but *SPRY2*) that were methylated in Eμ-TCL1 mice were also methylated (Fig. 1*A*) and silenced (Fig. 1*B*) in CLL patient samples. No increase in methylation was observed among patients with higher stage Rai disease or history of prior treatment. The patterns of aberrant methylation are tumor-type specific, as demonstrated by RLGS comparison of other mouse models of T/natural killer acute lymphoblastic leukemia (17) and *myc*-induced lymphoma (18) (Fig. 1*C*).

Early and Accumulated DNA Hypermethylation in Eμ-TCL1 CLL Progression. Next we investigated the frequency of altered DNA methylation in Eμ-TCL1 mice at different time points before development of CLL. We found that methylation increased over time in Eμ-TCL1 mice relative to WT animals, from 0.4%, 0.6%, 1.2%, and 1.9%, at 3, 5, 7, and 9 months respectively, to 3.9% in mice with advanced CLL (Fig. 2*A*). Similar results were also obtained from CD19-selected B cells from Eμ-TCL1 mice (0.4%, 1.0%, and 1.8% at 1, 5, and 7 months, respectively, and 4.1% in mice with advanced CLL; Table S1). Only minor age-dependent changes were found in the control mice, indicating that the increased frequency of DNA methylation is due to tumor-specific events (Fig. 2*A*). MassARRAY analysis was then performed to validate early aberrant DNA methylation in Eμ-TCL1 B cells. Consistent with the RLGS data, *Sox3*, *EphA7*, *Pcdh10*, and *Gpc6* were found to be methylated in CD19-positive B cells from Eμ-TCL1 mice starting at 5 months of age; *Dlx1* and *Id4* were only found to be methylated in mice with advanced disease as defined by elevated lymphocyte counts and/or palpable spleen (Fig. 2*B*). The repression of genes such as *Sox3* and *Gpc6* as determined by real-time RT-PCR correlated with the extent of increased DNA methylation detected in Eμ-TCL1 mice (Fig. 2*C*). Additionally, *GPC6* expression was reactivated in the B-lymphoblastic lymphoma Raji cell line and the WaC3CD5

CLL-like cell line by 5-aza-2′-deoxycytidine (5-aza-dC) (Fig. 2*D* and *E*), confirming the key role of methylation in silencing these genes.

Consistent with the increased aberrant DNA hypermethylation, elevated protein expression of the de novo DNA methyltransferases DNMT3A and DNMT3B, but not the maintenance methyltransferase DNMT1, was also observed in Eμ-TCL1 mouse B-lymphocytes over time (Fig. S1). However, this observation does not explain the targeted aberrant DNA methylation that occurs both in mouse and human CLL. While targeted DNA methylation has been demonstrated to lead to transcriptional silencing, as shown for Myc-induced transcriptional repression through recruitment of DNMTs (19), a growing body of evidence also supports that methylation-mediated silencing can occur following transcriptional repression (7, 20, 21). We therefore searched for differences in predicted transcription factor-binding sites within promoter regions (−2 kb to +1 kb) of methylated genes as compared to unmethylated genes. Using the Match program (22), the FOXD3 binding site (5′-A[AT]T[AG]TTTGTTT-3′) was found as the most significantly over-represented sequence (Fig. S2 *A* and *B*, $P = 0.007$). To validate the relevance of this site in B cells, chromatin immunoprecipitation (ChIP) was then performed to confirm the binding of FOXD3 within the predicted promoter regions in normal B cells. Of the 10 predicted targets in the methylated group that were tested, 9 showed FOXD3 binding by ChIP. In contrast, only 1 of the 10 unmethylated genes with a predicted FOXD3 binding sequence exhibited FOXD3 binding (Fig. 3*A*).

Early Loss of Transcription Activators in Eμ-TCL1 Mice. As described in Table S1, *Foxd3* was identified by RLGS to be methylated early in CLL progression in Eμ-TCL1 mice. Indeed, *Foxd3* methylation and down-regulation of *FOXD3* expression was detected both in CLL patient cells relative to normal cells, and in Eμ-TCL1 mice starting from 1-month-old mice relative to age-matched WT controls (Figs. 1*A* and 3 *B* and *C*). Putative FOXD3 target genes including *EphA7*, *Fign*, and *Phf2* also showed decreased expression in 1-month-old Eμ-TCL1 mice (Fig. 3 *D* and *E*). We hypothesized that this decreased expression is due to the loss of binding of FOXD3 within the promoter region. This hypothesis is supported by the transcription activator function of FOXD3, demonstrated by the increased promoter activity of both *Dlx1* and *EphA7* promoter luciferase constructs in Raji B cells with enforced FOXD3 expression (Fig. 4*A*). Consistent with these luciferase results, increased endogenous *DLX1* and *EPHA7* gene expression occurred in FOXD3-expressing Raji B cells following treatment with the hypomethylating agent 5-aza-dC. Because both *Dlx1* and *EphA7* are densely methylated in the Raji cell line, demethylation via 5-aza-dC treatment permits binding of FOXD3 and subsequent reactivation of *DLX1* and *EPHA7* (Fig. 4 *B* and *C*).

To test the effect of FOXD3 reduction on putative target genes, we used an shRNA approach. Because no B-cell lines without *Foxd3* DNA methylation could be found, the FOXD3-positive Jurkat T cell line was used for these experiments. While most of the methylated genes found in CLL cells are also methylated in Jurkat T cells, *DLX1* and *PHF2* were found to be expressed in these cells. Interestingly, transfection of *FOXD3* shRNA resulted in the silencing and methylation of both *DLX1* and *PHF2* following 17 days of culture (Fig. 4*D*). Similar results were also observed in the FOXD3 shRNA-transfected K562 chronic myelogenous leukemia cells (Fig. S3). Collectively, these data demonstrate that Foxd3 is silenced transcriptionally at a very early time point before development of disease and leads to silencing of many target genes dependent upon it for promoter activation.

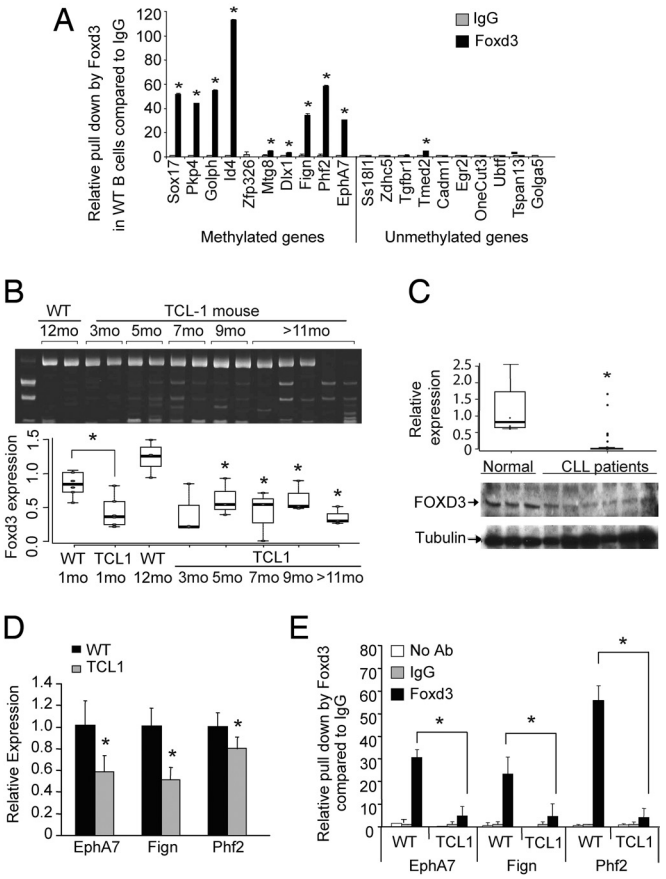

Fig. 3. High number methylated genes are downstream targets of repressed FOXD3 in CLL. (*A*) ChIP assay on 10 putative FOXD3 targets using 1-month-old WT mouse B-cell samples ($n = 3$). The relative FOXD3 pull down was normalized to a control IgG pull down for each gene analyzed. The extent of FOXD3 binding to methylated versus unmethylated target genes is significantly different by Fisher's Exact test ($P = 0.001$). (*B*) Methylation (Top) and expression (Bottom) of *Foxd3* measured by COBRA and SYBR-Green PCR was compared between $CD19^+$ B cells from WT and Eμ-TCL1 mice ($P < 0.05$ by Student *t* test). (*C*) *FOXD3* Expression in CLL patients. Top: TaqMan PCR results from 49 CLL samples compared with 4 normal $CD19^+$ B-cell samples ($P = 0.0002$ by Wilcoxon test). The box plot margins in (*B*) and (*C*) are the interquartile range with a thick line indicating the median. Each dot represents data from a single sample. Bottom: Foxd3 Immunoblot of B cells from 3 unaffected individuals and 6 CLL patients. (*D*) SYBR-Green PCR of FOXD3 target genes in splenic B cells from 1-month-old WT and TCL1 mice ($n = 3$, $P < 0.04$ by Student *t* test). (*E*) ChIP assay on splenic B cells from 1-month-old WT and TCL1 mice ($n = 3$, $P < 0.05$ by Student *t* test). The relative FOXD3 pull down was normalized to a control IgG pull down for each gene analyzed. Error bars, s.d.

FOXD3 Is Silenced by TCL1 Through a NF-κB p50:HDAC1 Repressor Complex. Silencing of *Foxd3* was first observed in 1-month-old Eμ-TCL1 mouse B cells, which is earlier than the occurrence of DNA methylation within the *Foxd3* promoter noted at 3 months of age. This observation suggests that enforced TCL1 expression in B cells may directly contribute to *FOXD3* transcriptional silencing. Consistent with this hypothesis, down-regulation of endogenous *Foxd3* (Fig. 5*A*) and decreased *FOXD3* promoter activity (Fig. 5*B*) was detected in EBV-immortalized human PBL lines expressing exogenous *TCL1*. We therefore interrogated mouse and human *Foxd3* promoters for transcription factor binding sites that could be regulated by signaling pathways relevant to TCL1 and to CLL pathogenesis. We identified a highly conserved putative NF-κB binding site in both the mouse and human *FOXD3* proximal promoters (Fig. 5*B*), prompting an investigation of the role for NF-κB in the regulation of *FOXD3*.

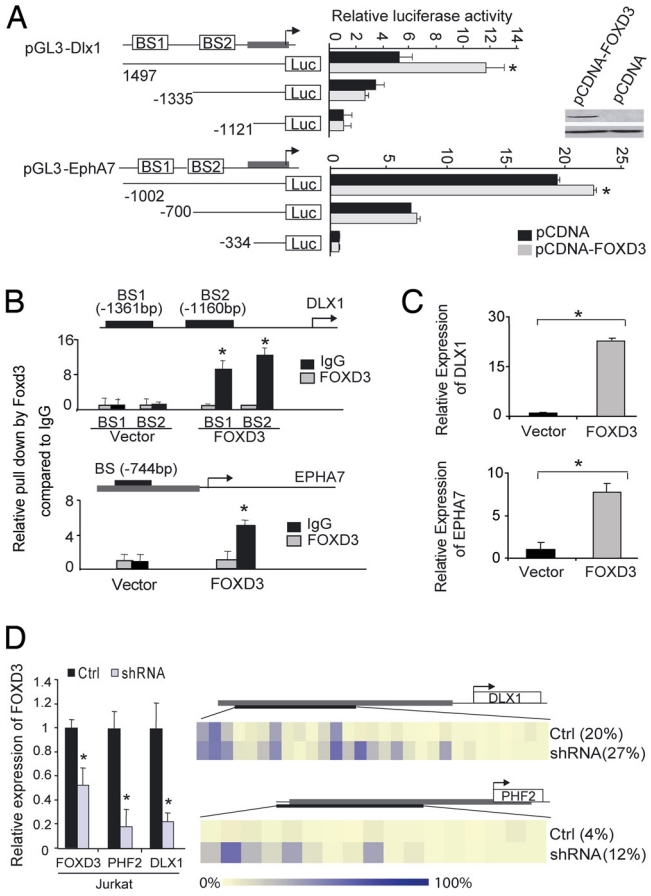

Fig. 4. Silenced and methylated FOXD3 targets in the knockdown lymphoblastic leukemia cell lines (*A*) Western blot (*Right*) shows FOXD3 expression in pcDNA3 vector and FOXD3 transfected Raji B cells. Promoter region schematics show 2 putative FOXD3 binding sites (BS1 and BS2) within the promoters of *Dlx1* and *EphA7*. A gray bar indicates the location of a CpG island. Relative luciferase activity was normalized to the pGL3-basic vector transfection control ($P < 0.05$). (*B*) ChIP assays for FOXD3 predicted binding sites (BS) in *DLX1* and *EPHA7* promoters in control-pcDNA (vector) or pcDNA-FOXD3 (FOXD3) transfected Raji cells after 0.5 μM 5aza-dC treatments for 3 days. Diagrams on the top indicate a represent pull-down DNA for the indicated binding sites. The relative pull down of FOXD3 was normalized by a control IgG pull down ($P < 0.001$). (*C*) SYBR-Green PCR of *DLX1* and *EPHA7* in control or FOXD3 transfected Raji cells after a 3-day treatment of 0.5 μM 5aza-dC. The relative expression of each gene was normalized to data from the first amplified sample ($P < 0.001$). (*D*) Downregulated (*Left*) and methylated (*Right*) of *DLX1*, and *PHF2* in Jurkat T-cells transfected with *FOXD3*-specific shRNA ($P < 0.001$). Schematics show the 5′ region of *DLX1* and *PHF2* genes. The black bars show the location of the analyzed amplicons. The average methylation percentage of both *DLX1* and *PHF2* amplicons is indicated. Error bars, s.d. Statistic analysis was done by Student *t* test.

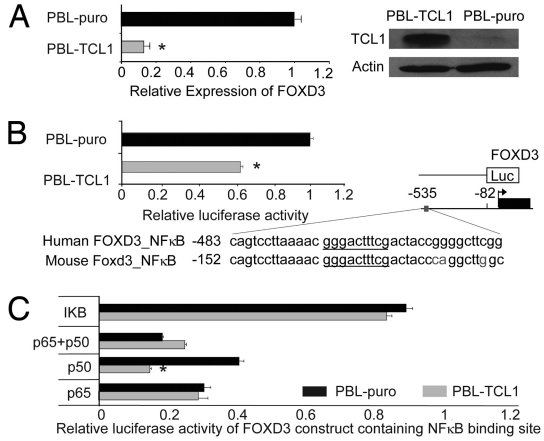

Fig. 5. Repressed *FOXD3* in NF-κB transfected *TCL1*-overexpressed PBL cell line. (*A*) Transformed PBL cells were transfected with a control vector (PBL-puro) or TCL1 (PBL-TCL1). *FOXD3* expression was analyzed by SYBR-Green PCR ($P = 0.007$). (*B*) Luciferase assay (*Top*) for *FOXD3* promoter activity using a *FOXD3* reporter containing the putative NF-κB binding site (gray square, the sequence is shown in *C*; $P = 0.005$). (*Bottom*) Identification of a conserved, putative NF-κB binding site in the mouse and human *Foxd3* promoters (underlined). (*C*) Luciferase assay for promoter activity using a *FOXD3* reporter construct and 500 ng of each NF-κB subunit expression vector. Cell lysates were collected after 48 h. Relative promoter activity was normalized to pCMV transfected PBL-puro cells. Results are averaged from triplicate assays. Error bars, s.d. ($P = 0.049$); all *P* values were calculated by Student *t* test.

Luciferase reporter assays in control or TCL1-expressing PBL lines indicated that *FOXD3* promoter activity was significantly repressed by a combination of TCL1 and NF-κB p50 subunit expression (Fig. 5*C*). Repeated electrophoretic mobility shift assays (EMSA) demonstrate stronger binding of NF-κB in extracts from CLL CD19+ selected cells compared with normal B cells, and the subsequent in vitro binding of p50 but not p65 to the *FOXD3* promoter (Fig. 6*A*). To identify other members of this DNA-binding complex, we performed EMSAs using antibodies to HDAC1 and HDAC3 based on their known role in *FOXD3* repression or as part of other NF-κB co-repressor complexes (23, 24). The results shown in Figure 6*A* demonstrate that HDAC1 appears to be part of this repressor complex. ChIP assays further confirm that p50 and HDAC1, but not HDAC3 or p65, are bound to the *FOXD3* promoter in CD19+ lymphocytes from both CLL patients and 1-month-old Eμ-TCL1 mice (Fig. 6*B*). In tolerant $CD4^+$ T-cells, it has been shown that the NF-κB p50 subunit is over-expressed in the nuclear fraction and represses transcription of IL-2 cytokine (25). We therefore tested whether similar silencing of *FOXD3* may occur in CLL cells. We demonstrate that nuclear but not cytoplasmic extracts of CLL contain higher p50 levels than normal B cells (Fig. 6*C*). This was also observed in the isolated B cells from 1-month-old Eμ-TCL1 mice (Fig. 6*D*). TCL1 is reported to directly interact with AKT and enhance its nuclear expression (26). This, coupled with the fact that phosphorylated AKT is enriched in the nucleus of CLL cells (Fig. 6*C*), led us to hypothesize that a similar association of TCL1 with the NF-κB p50 subunit also exists. Indeed, by forward and reverse immunoprecipitation, we demonstrated that TCL1 is directly associated with the NF-κB p50 subunit in CLL cells but not in normal B cells (Fig. 6*E*). Together, these results suggest transcriptional silencing of the NF-κB p50:HDAC1 co-repressor complex might be involved in the CLL development.

Discussion

In this study, we use extensive cross-species epigenetic analyses to identify a mechanism by which early transcriptional silencing events in the development of CLL occurs as a consequence of TCL1 over-expression. Specifically, we identify the embryonic stem cell gene *FOXD3* as 1 of the targets that is silenced early in B-cell transformation and precedes a cascade of gene silencing events detectable in mature CLL cells. Interestingly, we find that aberrant *TCL1* expression leads to *FOXD3* silencing through an NF-κB p50:HDAC1-mediated co-repressor complex. This unique co-repressor complex in TCL1-expressing B cells also is associated with increased nuclear p50 protein expression. Furthermore, in CLL cells but not normal B cells, we were able to demonstrate a direct interaction between TCL1 protein and the NF-κB p50 subunit. This abnormal p50:TCL1 association and subsequent forma-

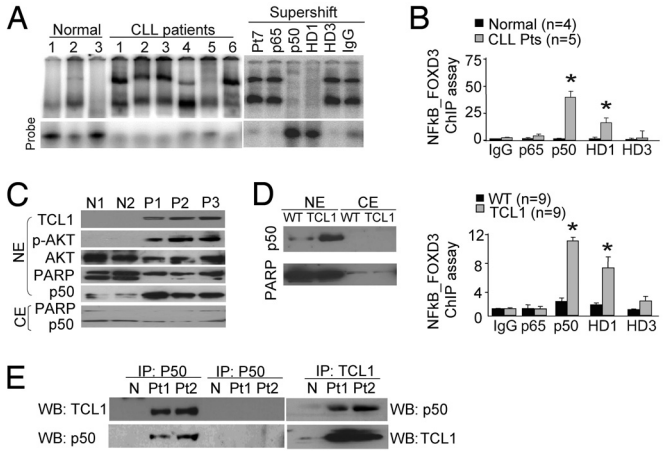

Fig. 6. *FOXD3* is repressed by NF-κB p50:HDAC1 complex in TCL1-expressing cells. (*A*) EMSA assays (*Left*) with the NF-κB binding sequence of the *FOXD3* promoter and nuclear extract from normal ($n = 3$) and CLL patient B-cell samples ($n = 6$). Supershift assay (*Right*) using B-cell samples from an additional patient with antibodies against p65, p50, HDAC1 (HD1), HDAC3 (HD3), and IgG. (*B*) ChIP assay (*Top*) surveying the *FOXD3* NF-κB promoter site in B cells from CLL patients and normal individuals. ChIP assay (*Bottom*) surveying the *Foxd3* NF-κB promoter site in splenic B cells from WT and 1-month-old TCL1 mice. The data were normalized to 1.0 by IgG pull down ($P < 0.05$ by Student *t* test). Error bars in the figures indicate s.d. (*C*) Western blots on 30 μg nuclear extract (NE) or cytoplasm extract (CE) from CLL patient and normal B-cell samples. (*D*) Western blots on 30 μg nuclear extract (NE) or cytoplasm extract (CE) of sorted B cells from 3 pooled 1-month-old TCL1 or WT mice. The nuclear protein PARP was used as an internal control. (*E*) Nuclear extract (500 μg) per sample from a normal donor or pooled from 2 CLL patient's B cells were immunoprecipitated (IP) with TCL1 (*Left*), p50 (*Right*) or control antibody against PARP, followed by Western blot analysis (WB) with antibodies against p50 or TCL1.

tion of a p50:HDAC1 co-repressor complex provides a target for CLL therapy.

The Eμ-TCL1 mouse studies described here demonstrate that transcriptional silencing represents an early event that is followed later by specific gene promoter methylation. While individual steps in this cascade of events need further investigation, a model has been proposed in colon and breast cancer where chromatin remodeling during the initial phases of gene silencing occurs before the DNA methylation (7, 20, 21). Our model demonstrates the direct contribution of the *TCL1* oncogene in the transcriptional silencing of the transcription factor *Foxd3* by an NF-κB p50:HDAC1 co-repressor complex. This subsequently triggers epigenetic silencing of downstream targets as a secondary event, leading to stable gene repression. Moreover, the fact that many Foxd3 target genes are also transcription factors implies a chain reaction, which may explain the accumulated number of hypermethylated genes in the Eμ-TCL1 transgenic mouse, and potentially in human CLL. This process may be favored by the de novo methyltransferases DNMT3A and 3B. The timing of specific gene methylation in the Eμ-TCL1 transgenic mouse is variable, and likely reflects differential promoter regulation by Foxd3 as well as the alteration of other contributing gene regulators in Eμ-TCL1 mice. Nonetheless, our studies in this CLL model demonstrate that transcriptional silencing of genes early and late in transformation occurs before development of DNA promoter methylation.

To date, the presence of *Foxd3* in normal mature B cells has not been reported and its function is uncharacterized. *Foxd3* is a member of forkhead-box (FOX) family transcription factors characterized by a monomeric DNA binding domain for nuclear localization and transcriptional regulation (27–30). No studies have related either *TCL1* or NF-κB co-repressor complexes to the silencing of *Foxd3*. Recruited HDAC1 by NF-κB p50/p50 homodimer forming the co-repressor complex, however, has been identified (23, 31). NF-κB repressor complex mediated transcriptional silencing has also been suggested to protect normal hepatocytes from TNF-α mediated apoptosis as a consequence of chronic inflammation (32). We therefore hypothesize that this co-repressor complex could provide a similar survival advantage for TCL1 over-expressing lymphocytes. Future studies examining the role of this NF-κB co-repressor complex and *Foxd3* silencing in transformation of CLL as well as other malignancies are warranted.

Our study also emphasizes the critical role of NF-κB in early epigenetic gene silencing of murine and human TCL1-positive CLL. A recent in vitro study suggests that TCL1 induces NF-κB activity by forming a complex of TCL1/NF-κB/CREB binding protein/p300 (33). Here we demonstrate that, in human CLL cells, TCL1 and p50 directly associate in the nucleus, similar to the interaction previously observed with TCL1 and AKT (26). With AKT, studies show that TCL1 both enhances activity of the kinase and also its nuclear translocation. Given that TCL1 was not identified in the p50:HDAC1 co-repressor complex, a selective subcellular localization role of TCL1 is a more likely mechanism that is currently under investigation in our laboratory. Given the importance of both co-repressor (data herein) and activating (34, 35) NF-κB complexes in the pathogenesis of CLL, there is strong rationale for the early introduction of agents that target the NF-κB pathway. In particular, small molecules derived to specifically inhibit the initiating p50:HDAC1 co-repressor complex would be of great interest for early use in the treatment of asymptomatic CLL to prevent development of the full disease phenotype.

Methodology

Mouse and Human Sample Preparation and Gene Expression Assays. C3H/B6 (Jackson Laboratories) and TCL1 transgenic mouse spleen CD19+ B cells were isolated by magnetic-activated cell sorting beads (Miltenyi Biotec). All animal experiments were performed under protocols approved by the Ohio State University Institutional Laboratory Animal Care and Use Committee. Human peripheral blood B cells were Rosette-Sep separated (Stem Cell Technologies), sampling was performed according to IRB approved protocols. Isolated high-molecular weight genomic DNA was used for RLGS, COBRA and MassARRAY analysis (Sequenom) as previously described (15). The construct of pJ6-Foxd3 was a kindly gift from R. Hromas. Foxd3 shRNA (Origene) transfected cells were selected by puromycin for 10 days. Cells were collected in 7 days after selection. Primer sequences used in gene expression assays are listed in Table S2.

Immunoprecipitation and Electrophoretic Mobility Shift Assays (EMSA). Co-immunoprecipitation (Co-IP) was performed by using 500 μg B-cell nuclear extract following manufacturer's instructions (ebioscience) using TCL1 and p50 antibodies (Santa Cruz Biotechnologies). Chromatin immunoprecipitaion (ChIP) was performed as described previously (36), the Ct values from IgG and FOXD3 pull-down were subtracted by the number obtained from 10× diluted input DNA. The relative pull-down of FOXD3 was then normalized by the subtracted Ct value of IgG (set as 1.0). EMSA was performed as previously described (37) with following modifications. The probe sequence was designed based on the putative NF-κB binding sequence (*ggggactttcg*) within *FOXD3* promoter. Oligonucleotides were labeled with [α-^{32}P]dCTP using the Nick Translation System (Invitrogen). The free probe was removed by purification in G50 Sephadex spin columns. The binding reaction was conducted at room temperature for 20 min with 5 μg nuclear extract and 20,000 dpm radiolabelled oligonucleotide probe. For supershift

GENETICS

assay, 1 μg antibody was added to the nuclear extract 15 min before addition of probe.

Cluster Analysis and Statistical Analysis. Hierarchical cluster analysis of samples was performed by applying phi-correlation (38) similarity metric with compact linkage method. All of the experiments were performed 3 times or more for the statistical analysis. Comparisons of 2 groups were performed by using non parametric Wilcox on rank sum test (39) and 2-tailed Student *t* test. Trend in methylation over time was evaluated by the Jonckheere-Terpstra test (44). Proportions between groups were compared using Fisher's exact test. All of the analyses were performed by *R 2.5.1* statistical program (http://www.r-project.org/). Error bars were developed by using mean ± standard error of the mean (s.e.m.) or by mean ± standard deviation (s.d.) of respective data.

ACKNOWLEDGMENTS. We thank all members of the Plass and Byrd laboratories for critical discussions and Dr. David Lucas for careful review of the final drafted manuscript. This work was supported by a T32 CA106196 fellowship in Cancer Genetics (to A.R.); National Cancer Institute Grants CA110496 (to J.C.B., C.P., and A.R.), A101956 (to C.P. and J.C.B.), CA81534 (to the CLL Research Consortium and to J.C.B., C. C.), and P30 CA16058 (to C.P. and J.C.B.); the Leukemia and Lymphoma Society (J.C.B. and C.P.); The D. Warren Brown Foundation (J.C.B.); and the Thompson family. C.P. was a Leukemia and Lymphoma Society scholar, and J.C.B. was a Leukemia and Lymphoma Society clinical scholar.

1. Jones PA, Baylin SB (2007) The epigenomics of cancer. *Cell* 128:683–692.
2. Weber M, et al. (2005) Chromosome-wide and promoter-specific analyses identify sites of differential DNA methylation in normal and transformed human cells. *Nat Genet* 37:853–862.
3. Suganuma T, Workman JL (2008) Crosstalk among histone modifications. *Cell* 135:604–607.
4. Preuss SB, et al. (2008) Multimegabase silencing in nucleolar dominance involves siRNA-directed DNA methylation and specific methylcytosine-binding proteins. *Mol Cell* 32:673–684.
5. Schones DE, Zhao K (2008) Genome-wide approaches to studying chromatin modifications. *Nat Rev Genet* 9:179–191.
6. Costello JF, et al. (2000) Aberrant CpG-island methylation has non-random and tumour-type-specific patterns. *Nat Genet* 24:132–138.
7. Bachman KE, et al. (2003) Histone modifications and silencing prior to DNA methylation of a tumor suppressor gene. *Cancer Cell* 3:89–95.
8. Chan TL, et al. (2006) Heritable germline epimutation of MSH2 in a family with hereditary nonpolyposis colorectal cancer. *Nat Genet* 38:1178–1183.
9. Gaudet F, et al. (2003) Induction of tumors in mice by genomic hypomethylation. *Science* 300:489–492.
10. Baylin SB, Ohm JE (2006) Epigenetic gene silencing in cancer - A mechanism for early oncogenic pathway addiction? *Nat Rev Cancer* 6:107–116.
11. Bichi R, et al. (2002) Human chronic lymphocytic leukemia modeled in mouse by targeted TCL1 expression. *Proc Natl Acad Sci USA* 99:6955–6960.
12. Johnson AJ, et al. (2006) Characterization of the TCL-1 transgenic mouse as a preclinical drug development tool for human chronic lymphocytic leukemia. *Blood* 108:1334–1338.
13. Browning RL, et al. (2007) Expression of TCL-1 as a potential prognostic factor for treatment outcome in B-cell chronic lymphocytic leukemia. *Leuk Res* 31:1737–1740.
14. Costello JF, Plass C, Cavenee WK (2002) Restriction landmark genome scanning. *Methods Mol Biol* 200:53–70.
15. Rush LJ, et al. (2004) Epigenetic profiling in chronic lymphocytic leukemia reveals novel methylation targets. *Cancer Res* 64:2424–2433.
16. Ehrich M, et al. (2005) Quantitative high-throughput analysis of DNA methylation patterns by base-specific cleavage and mass spectrometry. *Proc Natl Acad Sci USA* 102:15785–15790.
17. Yu L, et al. (2005) Global assessment of promoter methylation in a mouse model of cancer identifies ID4 as a putative tumor-suppressor gene in human leukemia. *Nat Genet* 37:265–274.
18. Opavsky R, et al. (2007) CpG island methylation in a mouse model of lymphoma is driven by the genetic configuration of tumor cells. *PLoS Genet* 3:1757–1769.
19. Brenner C, et al. (2005) Myc represses transcription through recruitment of DNA methyltransferase corepressor. *EMBO J* 24:336–346.
20. Jones PA, Baylin SB (2002) The fundamental role of epigenetic events in cancer. *Nat Rev Genet* 3:415–428.
21. Leu YW, et al. (2004) Loss of estrogen receptor signaling triggers epigenetic silencing of downstream targets in breast cancer. *Cancer Res* 64:8184–8192.
22. Kel AE, et al. (2003) MATCH: A tool for searching transcription factor binding sites in DNA sequences. *Nucleic Acids Res* 31:3576–3579.
23. Zhong H, May MJ, Jimi E, Ghosh S (2002) The phosphorylation status of nuclear NF-kappa B determines its association with CBP/p300 or HDAC-1. *Mol Cell* 9:625–636.
24. Dong J, Jimi E, Zhong H, Hayden MS, Ghosh S (2008) Repression of gene expression by unphosphorylated NF-kappaB p65 through epigenetic mechanisms. *Genes Dev* 22:1159–1173.
25. Grundstrom S, Anderson P, Scheipers P, Sundstedt A (2004) Bcl-3 and NFkappaB p50–p50 homodimers act as transcriptional repressors in tolerant CD4+ T cells. *J Biol Chem* 279:8460–8468.
26. Pekarsky Y, et al. (2000) Tcl1 enhances Akt kinase activity and mediates its nuclear translocation. *Proc Natl Acad Sci USA* 97:3028–3033.
27. Tompers DM, Foreman RK, Wang Q, Kumanova M, Labosky PA (2005) Foxd3 is required in the trophoblast progenitor cell lineage of the mouse embryo. *Dev Biol* 285:126–137.
28. Sutton J, et al. (1996) Genesis, a winged helix transcriptional repressor with expression restricted to embryonic stem cells. *J Biol Chem* 271:23126–23133.
29. Pan G, Li J, Zhou Y, Zheng H, Pei D (2006) A negative feedback loop of transcription factors that controls stem cell pluripotency and self-renewal. *FASEB J* 20:1730–1732.
30. Guo Y, et al. (2002) The embryonic stem cell transcription factors Oct-4 and FoxD3 interact to regulate endodermal-specific promoter expression. *Proc Natl Acad Sci USA* 99:3663–3667.
31. Williams SA, et al. (2006) NF-kappaB p50 promotes HIV latency through HDAC recruitment and repression of transcriptional initiation. *EMBO J* 25:139–149.
32. Oakley F, et al. (2005) Nuclear factor-kappaB1 (p50) limits the inflammatory and fibrogenic responses to chronic injury. *Am J Pathol* 166:695–708.
33. Pekarsky Y, et al. (2008) Tcl1 functions as a transcriptional regulator and is directly involved in the pathogenesis of CLL. *Proc Natl Acad Sci USA* 105:19643–19648.
34. Hewamana S, et al. (2008) The NF-{kappa}B subunit Rel A is associated with in vitro survival and clinical disease progression in chronic lymphocytic leukemia and represents a promising therapeutic target. *Blood* 111:4681–4689.
35. Furman RR, Asgary Z, Mascarenhas JO, Liou HC, Schattner EJ (2000) Modulation of NF-kappa B activity and apoptosis in chronic lymphocytic leukemia B cells. *J Immunol* 164:2200–2206.
36. Tada Y, et al. (2006) Epigenetic modulation of tumor suppressor CCAAT/enhancer binding protein alpha activity in lung cancer. *J Natl Cancer Inst* 98:396–406.
37. Chen CH, et al. (2005) Bidirectional signals transduced by DAPK-ERK interaction promote the apoptotic effect of DAPK. *EMBO J* 24:294–304.
38. Cohen J (1983) in *Applied Multiple Regression/Correlation Analysis for the Behavioral Sciences* (Lawrence Erlbum Associates Inc., Hillsdale, NJ), 2nd Ed.
39. Hollander M (1999) in Nonparametric Statistical Methods (John Wiley & Sons Inc., NY), 2nd Edition.
40. Huttenhofer A, Brosius J, Bachellerie JP (2002) RNomics: Identification and function of small, non-messenger RNAs. *Curr Opin Chem Biol* 6:835–843.
41. Wingender E, et al. (2000) TRANSFAC: An integrated system for gene expression regulation. *Nucleic Acids Res* 28:316–319.
42. Thompson JD, Higgins DG, Gibson TJ (1994) CLUSTAL W: Improving the sensitivity of progressive multiple sequence alignment through sequence weighting, position-specific gap penalties, and weight matrix choice. *Nucleic Acids Res* 22:4673–4680.
43. Jin VX, Rabinovich A, Squazzo SL, Green R, Farnham PJ (2006) A computational genomics approach to identify cis-regulatory modules from chromatin immunoprecipitation microarray data–a case study using E2F1. *Genome Res* 16:1585–1595.
44. Said JW, et al. (2001) TCL1 oncogene expression in B cell subsets from lymphoid hyperplasia and distinct classes of B cell lymphoma. *Lab Invest* 81:555–564.